JOM, Vol. 71, No. 9, 2019
https://doi.org/10.1007/s11837-019-03578-6

Effect of Roasting Characteristics of Vanadium-Rich Slag on Its Vanadium Leaching Behavior

WEI LI,[1,2] HAIYAN ZHENG,[1] and FENGMAN SHEN[1]

1.—School of Metallurgy, Northeastern University, Shenyang 110819, Liaoning, China. 2.—e-mail: lw_neu@126.com

The effect of the roasting characteristics of vanadium-rich slag on its vanadium leaching behavior was investigated to enable its effective utilization. Thermodynamic analysis of the sodium roasting of vanadium-rich slag was performed for the first time. The effect of the roasting temperature, roasting time, quantity of sodium carbonate (Na_2CO_3) added, and particle size of the raw material on the vanadium leaching was studied. The results showed that the oxidation reactions of vanadium oxides, fayalite (Fe_2SiO_4), and vanadium-iron spinel (FeV_2O_4), and the formation of sodium vanadate were feasible within the roasting temperature range. The sodium roasting was significant for the subsequent vanadium leaching process. The optimum process conditions for sodium roasting were roasting temperature of 850°C, roasting time of 60 min, Na_2CO_3 addition of 20%, and particle size of − 74 μm, resulting in an ideal vanadium leaching ratio. The results of the current study provide experimental evidence to establish a correlation between the roasting characteristics of vanadium-rich slag and its vanadium leaching behavior, as well as a theoretical and technical basis for effective utilization of vanadium-rich slag.

INTRODUCTION

Vanadium is a strategic metal that is widely used in many fields, including the steel, aerospace, and chemical industries, due to its excellent properties.[1–5] China is a country that is rich in vanadium resources.[6–8] Nearly 88% of the vanadium in the world is extracted from vanadium titanomagnetite. Vanadium titanomagnetite is abundant in China, where the ore in the Panzhihua–Xichang area alone accounts for 95% of total vanadium titanomagnetite resources.[9–12] Comprehensive utilization of vanadium titanomagnetite increases its value and has been extensively developed in recent years.

At present, the blast furnace (BF) process is the main operating method used for melting vanadium titanomagnetite. During the BF process, Fe and V are both reduced to hot metal, while most of the Ti is not reduced, remaining in the BF slag. During the basic oxygen furnace (BOF) process, the V in the hot metal is oxidized and enriched into the slag, which is called vanadium-rich slag because of its high vanadium content. The processes used to extract vanadium from the vanadium-rich slag mainly include oxidation roasting, leaching, extraction, and precipitation, among which the most important procedures are oxidation roasting and leaching. The aim of oxidation roasting is to transfer insoluble vanadium compounds into soluble vanadates.[13–18] Oxidation roasting of vanadium spinel and vanadium slag has been intensively studied.[19–25] Li et al.[19] performed a direct roasting and soda leaching process to extract vanadium from high-calcium vanadium slag. Yu et al.[21] examined whether vanadium-rich phases could be obtained in converter slags. However, it remains difficult to control the process parameters during the sodium roasting process, as interaction reactions or mutual influences among components affect the vanadium recovery ratio. Furthermore, there is no research regarding the relationship between the oxidation roasting and leaching behavior, indicating the need to investigate the effect of the roasting characteristics of vanadium-rich slag on its vanadium leaching behavior.

In the work presented herein, thermodynamic calculations and analysis were carried out first, then the effects of various factors during the

 (Published online June 6, 2019)

roasting of vanadium-rich slag on its leaching behavior were further investigated. The results provide experimental evidence to establish a correlation between its roasting characteristics and vanadium leaching behavior, as well as a theoretical and technical basis for effective utilization of vanadium-rich slag.

EXPERIMENTAL PROCEDURES

Materials

The vanadium-rich slag used in this study was obtained from the Panzhihua Iron & Steel Group of China. Its chemical composition is presented in Table I. The phase composition of the slag was investigated by x-ray diffraction (XRD) analysis (Fig. 1), indicating that the main phases present were vanadium-iron spinel (FeV_2O_4), fayalite (Fe_2SiO_4), and pyroxene ($CaMgSi_2O_6$). Analytically pure sodium carbonate (Na_2CO_3) was used as the sodium agent in this work.

Experimental Procedures

The vanadium-rich slag and sodium agent were homogeneously mixed in a ball mill for 60 min before the oxidation roasting process. The oxidation roasting experiments were performed in a muffle furnace with a temperature control programmer. When the desired temperature was achieved, the sample was placed in the muffle furnace and roasted under air atmosphere for the required time. Once the oxidation roasting experiment had finished, the sample was removed from the muffle furnace quickly and cooled to room temperature. In a typical experiment, the roasting conditions were roasting temperature of 850°C, roasting time of 60 min, 20% Na_2CO_3 addition, and particle size of − 200 mesh (− 74 μm), with one parameter being changed while the others were kept constant.

During the water leaching process, 2 g of roasted vanadium-rich slag was leached under constant conditions. Based on our previous studies, the leaching temperature, leaching time, and liquid–solid ratio were set at 90°C, 45 min, and 5:1 mL/g, respectively. The slurry was separated via centrifuge, and the residue was washed several times with distilled water. To guarantee the accuracy, each experiment was repeated two times and the mean used to reduce the deviation. The vanadium content of the primary and residual slags was analyzed by inductively coupled plasma-optical emission spectrometry (ICP-OES). The phase composition of the roasted vanadium-rich slag was determined by XRD analysis.

The leaching ratio of vanadium was defined as

$$\text{Leaching ratio} = \frac{m_1 w_1 - m_2 w_2}{m_1 w_1} \times 100\%, \quad (1)$$

where m_1 and m_2 are the masses of roasted vanadium-rich slag before and after leaching, respectively (g), and w_1 and w_2 are the mass fractions of vanadium in the roasted vanadium-rich slag before and after leaching, respectively (%).

THERMODYNAMIC ANALYSIS

Oxidation Reaction

The standard Gibbs free energies at the temperature of the oxidation reactions were calculated using FactSage thermodynamics software and are shown in Fig. 2. Figure 2a shows that the main reactions were exothermic, occurring with difficulty as the temperature is increased. The stability order is vanadium oxide (VO) > vanadium trioxide (V_2O_3) > vanadium tetraoxide (V_2O_4) > vanadium pentoxide (V_2O_5), and the final oxidation product is V_2O_5.

The vanadium-rich slag was primarily composed of Fe_2SiO_4 and FeV_2O_4. The standard Gibbs free energies for the oxidation reactions of Fe_2SiO_4 are shown in Fig. 2b. The oxidation reactions of Fe_2SiO_4 occur over a wider range of temperature, and the standard Gibbs free energies for the generation of ferroferric oxide (Fe_3O_4) and silicon dioxide (SiO_2)

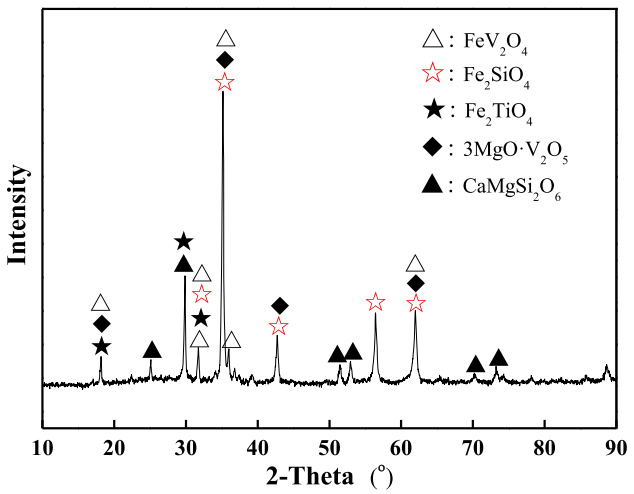

Fig. 1. XRD pattern of vanadium-rich slag.

Table I. Chemical composition of vanadium-rich slag used in this study (wt.%)

Fe_2O_3	V_2O_5	SiO_2	TiO_2	MnO	MgO	CaO	Al_2O_3	Others
37.38	16.30	14.09	12.09	8.16	4.01	1.98	3.42	2.57

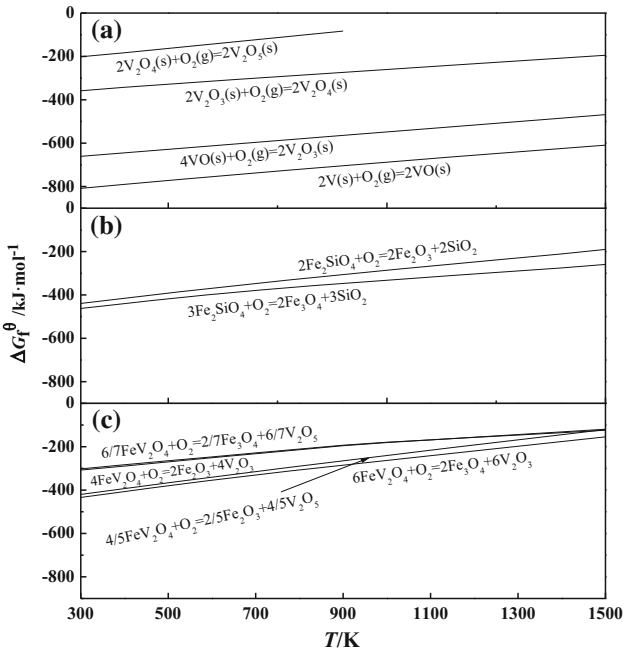

Fig. 2. Standard Gibbs free energy for the oxidation reaction: (a) vanadium oxides, (b) Fe_2SiO_4, and (c) FeV_2O_4.

are lower. Fe_3O_4 will be further oxidized to ferric oxide (Fe_2O_3), and the final phases are Fe_2O_3 and SiO_2. The above reactions occur from the thermodynamic point of view, but the factor limiting such oxidation at low temperature is the kinetics, so the reactions that occur will depend on the coupled result of the controlling thermodynamics and kinetics.

The standard Gibbs free energies for the oxidation reactions of FeV_2O_4 are shown in Fig. 2c. The reactions occur across a wide range of temperature. FeV_2O_4 reacts with oxygen (O_2) to form V_2O_3 initially, although the reactions occur with difficulty as the temperature is increased. Moreover, V_2O_3 is further oxidized to V_2O_5. Therefore, the final phases of the oxidation of FeV_2O_4 are V_2O_5 and Fe_2O_3.

Formation of Sodium Vanadate

The primary aim of sodium roasting of vanadium-rich slag is to transfer insoluble vanadium compounds into soluble vanadates under high-temperature conditions to react with sodium carbonate to form sodium vanadates. Sodium orthovanadate (Na_3VO_4), sodium metavanadate ($NaVO_3$), and sodium pyrovanadate ($Na_4V_2O_7$) are the common vanadates; their standard Gibbs free energies versus temperature were calculated using FactSage thermodynamics software (Fig. 3). The reaction for the formation of $NaVO_3$ is the most likely to occur because of its lowest standard Gibbs free energy. $NaVO_3$ is the most stable when sufficient Na_2CO_3 and O_2 are present.

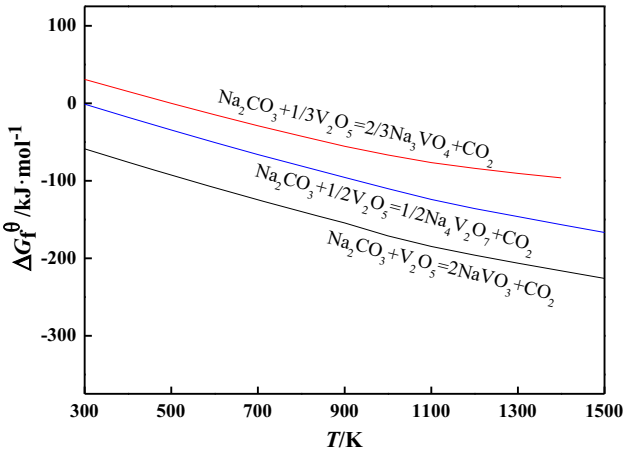

Fig. 3. Standard Gibbs free energy for formation of vanadate.

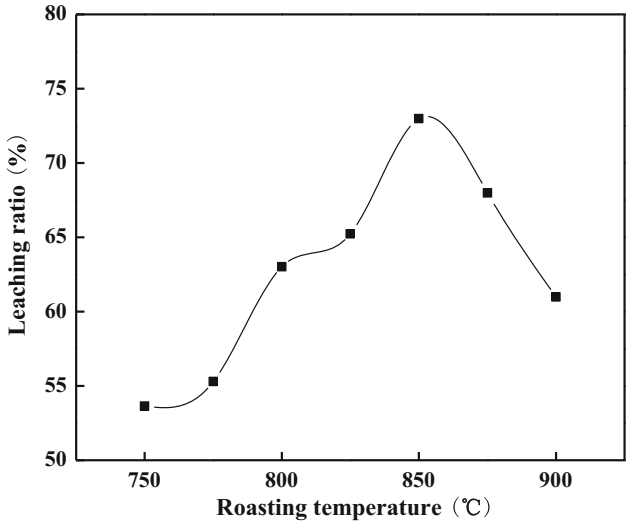

Fig. 4. Influence of roasting temperature on vanadium leaching ratio.

RESULTS AND DISCUSSION

Effect of Roasting Temperature

The effect of the roasting temperature on the vanadium extraction was investigated from 750°C to 900°C (Fig. 4). The vanadium leaching ratio increased gradually, reaching a maximum value at 850°C. This indicates that the roasting temperature had a significant influence on the formation of sodium vanadate during the roasting process. However, the vanadium leaching ratio decreased when the roasting temperature was increased further.

The XRD patterns of vanadium-rich slag roasted at different temperatures are shown in Fig. 5. When the roasting temperature was 750°C, FeV_2O_4 was still present, meaning that low-valence vanadium was not completely oxidized. At 850°C, the intensity and number of $NaVO_3$ peaks increased. The slag roasted at 900°C showed peaks for calcium metavanadate (CaV_2O_6), which will result in a decrease of the vanadium leaching ratio in the subsequent

leaching process. The corresponding reaction is as follows:

$$V_2O_5 + CaO = CaV_2O_6 \quad (2)$$

Semiquantitative XRD analysis was also carried out (Fig. 6). The relative content of Fe_2O_3 in Fig. 6a increased as the roasting temperature was increased for constant roasting time. Figure 6b shows that the amount of $NaVO_3$ increased with the roasting temperature up to 850°C. If the amount of $NaVO_3$ is high, more vanadium could be leached in the subsequent leaching process, corresponding to the increased vanadium leaching ratio observed in Fig. 4. However, when the roasting temperature exceeded 850°C, the amount of $NaVO_3$ decreased, which is consistent with the decreased vanadium leaching ratio in the subsequent leaching process seen in Fig. 4.

Figure 6c shows that the relative content of CaV_2O_6 increased with increase of the roasting temperature for constant roasting time, particularly at higher temperatures. As is known, CaV_2O_6 is difficult to dissolve in water during the leaching process, decreasing the vanadium leaching ratio at higher temperatures. These results further confirm that the roasting temperature had an important effect on the roasting characteristics of the vanadium-rich slag.

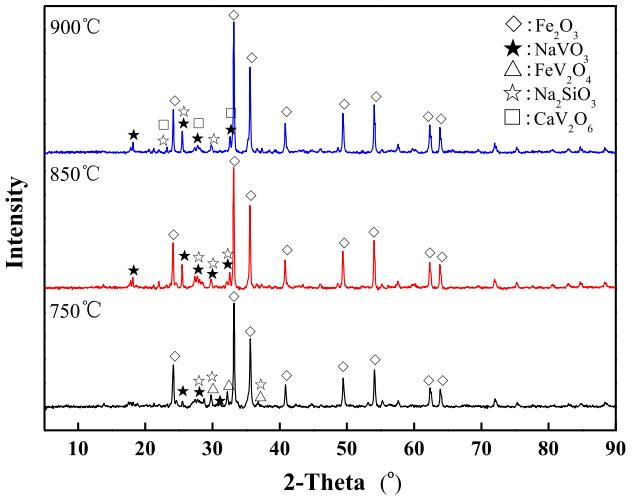

Fig. 5. XRD patterns of vanadium-rich slag roasted at different temperatures.

Effect of Roasting Time

To study the effect of the roasting time on the vanadium extraction, it was varied from 30 min to 180 min with roasting temperature of 850°C. The results (Fig. 7) indicated that the vanadium

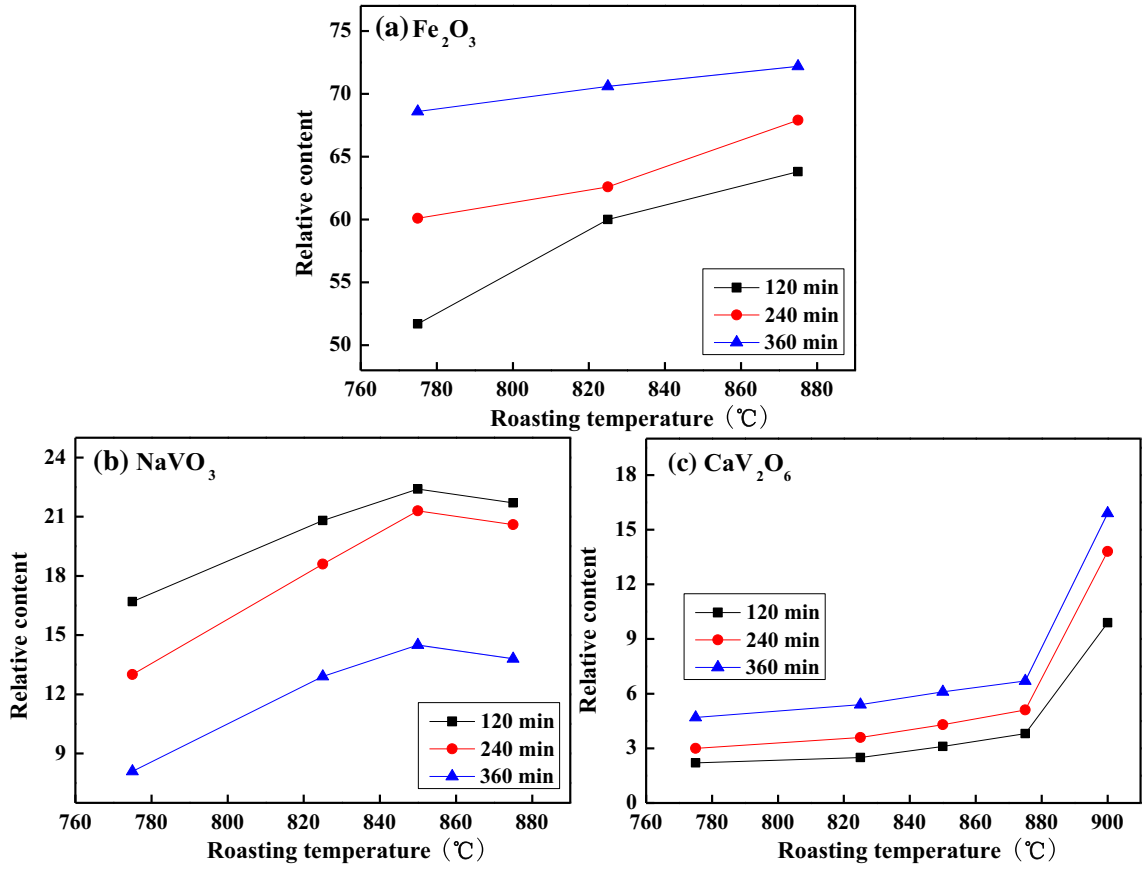

Fig. 6. Semiquantitative XRD analysis of roasted vanadium-rich slag: (a) Fe_2O_3, (b) $NaVO_3$, and (c) CaV_2O_6.

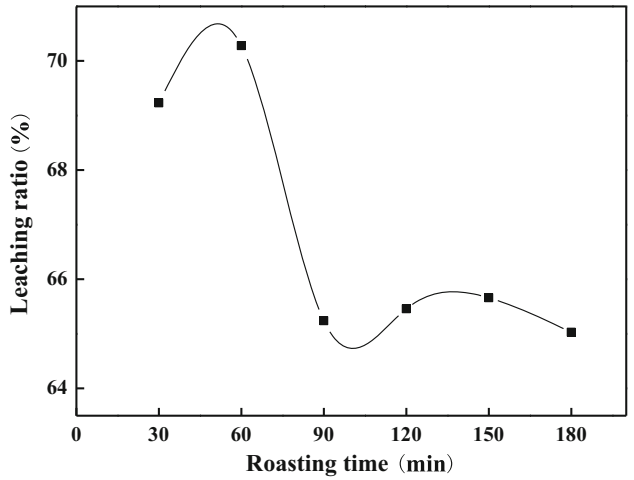

Fig. 7. Influence of roasting time on vanadium leaching ratio (roasting temperature: 850°C).

leaching ratio increased with the roasting time, reaching a peak value at 60 min but decreasing thereafter. When the roasting time was 120 min, the leaching ratio was 65.46%. When the roasting time exceeded 120 min, for example, at 150 min, the leaching ratio was 65.66%, remaining almost unchanged.

To further clarify the mechanism of sodium roasting of vanadium-rich slag, vanadium-rich slag roasted for different times was subjected to XRD analysis (Supplementary Fig. S1). When the roasting time was 60 min, diffraction peaks for FeV_2O_4 were not detected. When the roasting time was increased to 90 min, CaV_2O_6 appeared, causing the vanadium leaching ratio to decrease.

Effect of Na_2CO_3 Addition

The effect of Na_2CO_3 addition on the extraction of vanadium was investigated in the range from 14% to 26% at 850°C for 60 min. The leaching conditions were the same as mentioned above, and the results are shown in Supplementary Fig. S2. The vanadium leaching ratio increased as the amount of Na_2CO_3 added was increased from 14% to 20%, but decreased when more Na_2CO_3 was added. Supplementary Fig. S3 depicts the XRD patterns of vanadium-rich slag roasted with different Na_2CO_3 additions, showing that $NaAlSi_3O_8$ was detected when the amount of Na_2CO_3 added was increased from 20% to 23%. This primarily occurs because the vanadium was encased by sintered matter, decreasing the vanadium leaching ratio.

Effect of Particle Size of Raw Material

The effect of the particle size of the raw material on the extraction of vanadium was investigated from + 100 to − 200 mesh at 850°C for 60 min with 20% Na_2CO_3 addition. Supplementary Fig. S4 shows that the vanadium leaching ratio increased as the particle size of the raw material was decreased. When the particle size of the raw material was varied from 100–150 to − 200 mesh, the vanadium leaching ratio did not change significantly.

The XRD patterns of roasted vanadium-rich slag with different particle sizes are shown in Supplementary Fig. S5. For the + 100 mesh particle size, the diffraction peaks of FeV_2O_4 were still observed while the diffraction peaks of $NaVO_3$ were weak. For the particle size of − 200 mesh (− 74 μm), the diffraction peaks of FeV_2O_4 nearly disappeared and the diffraction peaks of $NaVO_3$ became strong, resulting in the increased vanadium leaching ratio.

CONCLUSION

The effects of the roasting characteristics of vanadium-rich slag on its vanadium leaching behavior were systematically investigated. The following conclusions can be drawn:

1. The oxidation reactions of the vanadium oxides, Fe_2SiO_4, and FeV_2O_4, were feasible within the studied roasting temperature range. At the experimental roasting temperature, the reaction for formation of water-soluble sodium vanadate was feasible when Na_2CO_3 was used as the sodium agent, occurring more easily with increased temperature.
2. Sodium roasting was significant for the vanadium extraction process. The vanadium leaching ratio initially increased with increasing roasting temperature below 850°C, but decreased thereafter. The vanadium leaching ratio increased with extension of the roasting time up to 60 min, then decreased before leveling off. The vanadium leaching ratio exhibited an upward trend as the amount of Na_2CO_3 added was increased up to 20%, leveling off thereafter. As the particle size of the raw material was decreased, the vanadium leaching ratio showed an upward trend, reaching a maximum at the particle size of − 74 μm.
3. The optimum process conditions for sodium roasting were roasting temperature of 850°C, roasting time of 60 min, Na_2CO_3 addition of 20%, and particle size of − 74 μm. Under these roasting conditions, the vanadium leaching ratio reached 84.61% at the constant leaching conditions (leaching temperature 90°C, leaching time 45 min, liquid–solid ratio 5:1 mL/g). In practical industrial production, the roasting system should be optimized as much as possible to improve the vanadium leaching efficiency.

ACKNOWLEDGEMENTS

The authors gratefully acknowledge support from the Fundamental Research Funds for the Central Universities (N182503032), Postdoctoral International Exchange Program (Dispatch Project), and

National Natural Science Foundation of China (51774071 and 51374061).

ELECTRONIC SUPPLEMENTARY MATERIAL

The online version of this article (https://doi.org/10.1007/s11837-019-03578-6) contains supplementary material, which is available to authorized users.

REFERENCES

1. G.M. Zhang, K.Q. Feng, and H.F. Yue, *JOM* 68, 2525 (2016).
2. S. Wang, Y.F. Guo, T. Jiang, L. Yang, F. Chen, F.Q. Zheng, X.L. Xie, and M.J. Tang, *JOM* 69, 1646 (2017).
3. Y.M. Zhang, S.X. Bao, T. Liu, T.J. Chen, and J. Huang, *Hydrometallurgy* 109, 116 (2011).
4. K. Mazurek, *Hydrometallurgy* 134, 26 (2013).
5. R.R. Moskalyk and A.M. Alfantazi, *Miner. Eng.* 16, 793 (2003).
6. T. Hu, X.W. Lv, and C.G. Bai, *Steel Res. Int.* 87, 494 (2016).
7. H.M. Long, T.J. Chun, P. Wang, Q.M. Meng, Z.X. Di, and J.X. Li, *Metall. Mater. Trans. B* 47, 1765 (2016).
8. L.S. Zhao, L.N. Wang, T. Qi, D.S. Chen, H.X. Zhao, and Y.H. Liu, *Hydrometallurgy* 149, 106 (2014).
9. S. Wang, Y.F. Guo, T. Jiang, L. Yang, F. Chen, F.Q. Zheng, X.L. Xie, and M.J. Tang, *JOM* 69, 1646 (2017).
10. X.W. Lv, Z.G. Lun, J.Q. Yin, and C.G. Bai, *ISIJ Int.* 53, 1115 (2013).
11. T. Hu, X.W. Lv, C.G. Bai, Z.G. Lun, and G.B. Qiu, *Metall. Mater. Trans. B* 44, 252 (2013).
12. S. Samanta, S. Mukherjee, and R. Dey, *JOM* 67, 467 (2015).
13. M.Y. Wang, P.F. Xian, X.W. Wang, and B.W. Li, *JOM* 67, 369 (2015).
14. X.S. Li, B. Xie, G.E. Wang, and X.J. Li, *Trans. Nonferr. Metals Soc. China* 21, 1860 (2011).
15. M. Li, H. Du, S.L. Zheng, S.N. Wang, Y. Zhang, B. Liu, A.B. Dreisinger, and Y. Zhang, *JOM* 69, 1970 (2017).
16. G.Q. Zhang, T.A. Zhang, G.Z. Lv, Y. Zhang, Y. Liu, and W.G. Zhang, *JOM* 68, 577 (2016).
17. M.S. Villarreal, B.I. Kharisov, L.M. Torres-Martínez, and V.N. Elizondo, *Ind. Eng. Chem. Res.* 38, 4624 (1999).
18. R.R. Moskalyk and A.M. Alfantazi, *Miner. Eng.* 16, 793 (2003).
19. X.S. Li and B. Xie, *Int. J. Miner. Metall. Mater.* 19, 595 (2012).
20. C.P.J.V. Vuuren and P.P. Stander, *Thermochim. Acta* 254, 227 (1995).
21. L. Yu, Y.C. Dong, G.Z. Ye, and S.C. Du, *Ironmak. Steelmak.* 34, 131 (2007).
22. X.Y. Chen, X.Z. Lan, Q.L. Zhang, H.Z. Ma, and J. Zhou, *Trans. Nonferr. Metals Soc. China* 20, 123 (2010).
23. K. Yang, X.Y. Zhang, X.D. Tian, Y.L. Yang, and Y.B. Chen, *Hydrometallurgy* 103, 7 (2010).
24. Z.W. Pan, D.W. Wang, H. Du, G. Chen, S.L. Zheng, and J. Cent, *South Univ.* 24, 2171 (2014).
25. X.J. Zhai, Y. Fu, X. Zhang, L.Z. Ma, and F. Xie, *Hydrometallurgy* 99, 189 (2009).